

Momentum Distribution and Renormalization Factor in Sodium and the Electron Gas

Simo Huotari,^{1,2} J. Aleksi Soininen,² Tuomas Pylkkänen,^{1,2} Keijo Hämäläinen,² Arezki Issolah,³ Andrey Titov,⁴ Jeremy McMinis,⁵ Jeongnim Kim,⁵ Ken Esler,⁵ David M. Ceperley,⁵ Markus Holzmann,⁶ and Valerio Olevano⁴

¹European Synchrotron Radiation Facility, B.P. 220, F-38043 Grenoble, France

²Department of Physics, P. O. Box 64, FI-00014, University of Helsinki, Finland

³Université de Tizi-Ouzou, Campus de Hasnaoua, 15000 Tizi-Ouzou, Algeria

⁴Institut Néel, CNRS & UJF, F-38042 Grenoble, France

⁵Dept. of Physics and NCSA, U. of Illinois at Urbana-Champaign, Urbana, IL 61801, USA

⁶LPTMC, UPMC-CNRS, Paris, France, and LPMCMC, UJF-CNRS, F-38042 Grenoble, France

(Dated: October 24, 2018)

We present experimental and theoretical results on the momentum distribution and the quasiparticle renormalization factor in sodium. From an x-ray Compton-profile measurement of the valence-electron momentum density, we derive its discontinuity at the Fermi wavevector. This yields an accurate measure of the renormalization factor that we compare with quantum Monte Carlo and G_0W_0 calculations performed both on crystalline sodium and on the homogeneous electron gas. Our calculated results are in good agreement with the experiment.

PACS numbers: 71.10.-w, 78.70.Ck, 71.20.Dg, 02.70.Ss

Introduction The homogeneous electron gas (HEG), also known as jellium, is one of the most fundamental models in condensed matter physics [1]. It is one of the simplest many-body systems which can still describe several properties of real solids, especially of the alkali metals. For almost half a century, the accurate description of many-body correlation effects has challenged quantum many-body theory and HEG is the canonical workbench to test different theoretical methods [2–8]. Although the exact analytic solution of the many-body problem in HEG is still unknown, today quantum Monte Carlo (QMC) calculations are widely accepted to provide the most reliable results on e.g. the correlation energy. The situation is less clear concerning spectroscopic quantities such as the momentum distribution, $n(p)$. The accuracy of the theoretical methods in this respect is not well understood, different approaches yielding a wide range of varying results. This fundamental issue has remained unresolved, mainly due to a lack of accurate, bulk-sensitive and unambiguous experimental probes that could be used to compare the theories with.

Experimentally, one of nature’s closest realizations of HEG is formed by the valence electrons in alkali metals, especially Na. Here, we present very accurate experimental and theoretical results on the electron-momentum distribution of Na. The single occupied valence band of Na has an almost spherical Fermi surface and its properties in ambient conditions with a density parameter $r_s = 3.99$ can be directly compared with theoretical results on HEG. In particular, we obtain a precise experimental reference value for the quasiparticle renormalization factor, Z_{k_F} , which characterizes the discontinuity of the momentum distribution at the Fermi surface at this density [1].

From the Compton profile (CP) measured by inelastic x-ray scattering experiments on bulk sodium, we derive

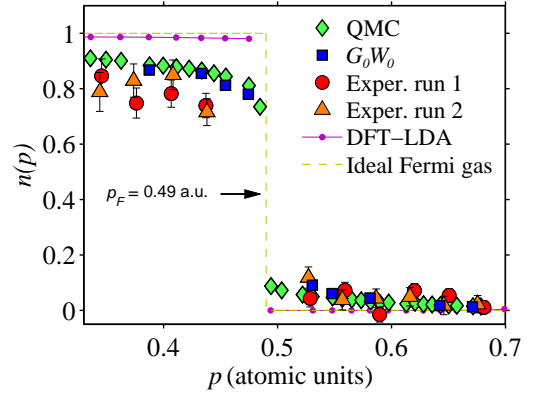


FIG. 1: (Color online) The momentum distribution of Na determined by experiment, QMC using Slater-Jastrow wavefunctions, G_0W_0 , and DFT-LDA calculations. The ideal-Fermi gas step function is also shown.

$n(p)$ and obtain $Z_{k_F}^{\text{Na}} = 0.58(7)$. Compared to previous experiments [9], our experimental resolution provides a clear observation of the discontinuity at the Fermi surface in a direct and model-independent way.

We compare our experimental results to theoretical calculations using QMC and G_0W_0 methods, both done for HEG and for solid Na taking into account the electron-electron interaction and band-structure effects. Our calculations confirm the jellium-like behavior of Na and allow us to quantify the small band-structure-induced deviations from HEG. Finally, we compare the results with other many-body approximations applied to HEG in literature [2–8] (Table I). Unless explicitly specified, we use atomic units (a.u.).

Theory The momentum distribution per spin state, $n(p)$ (see Fig. 1), is one of the basic many-body observables where the Pauli principle for fermions is directly

Technique	ζ^{Na}	$Z_{k_F}^{\text{Na}}$	$Z_{k_F}^{\text{HEG}}$
Experiment	0.57(7)	0.58(7)	
QMC-SJ	0.68(2)	0.70(2)	0.69(1)
QMC-BF			0.66(2)
G_0W_0	0.64(1)	0.65(1)	0.64 [2]
GW			0.793 [6]
RPA (on-shell)			0.45 [4, 5]
exp S_2			0.59 [4]
EPX			0.61 [8]
Lam			0.615 [5]
FHNC			0.71 [7]

TABLE I: Our results for ζ and Z_{k_F} of Na and HEG at $r_s = 4.0$: experimental value compared to G_0W_0 , as well as QMC results based on Slater-Jastrow (QMC-SJ) and more precise backflow (QMC-BF) wavefunctions. Various theoretical values of HEG from literature are also quoted.

visible. It is the probability to observe an electron with momentum p . For a non-interacting Fermi gas at zero temperature, $n(p)$ is 1 for p below the Fermi momentum p_F and 0 above, i.e. $n(p) = \theta(p_F - p)$ with a discontinuity $\zeta = n(p_F^-) - n(p_F^+) = 1$ occurring at the Fermi surface. For a non-interacting crystalline system, the electrons occupy Bloch wavefunctions, $\phi_{\nu\mathbf{k}}(\mathbf{r}) = \sum_{\mathbf{G}} \tilde{\phi}_{\nu\mathbf{k}}^{\mathbf{G}} e^{i(\mathbf{k}+\mathbf{G})\mathbf{r}}$, where \mathbf{k} is the crystal momentum, ν the band index, and \mathbf{G} are reciprocal lattice vectors. For systems like Na with one valence band ($\nu = 1$) whose Fermi surface is entirely contained within the first Brillouin zone (1BZ), the band structure reduces the discontinuity of the momentum distribution, $\zeta = |\tilde{\phi}_{\nu=1, \mathbf{k}_F}^{\mathbf{G}=0}|^2 < 1$. From a density-functional theory calculation within the local-density approximation (DFT-LDA) for Na, we obtain $\zeta_{\text{DFT}}^{\text{Na}} = 0.98(1)$. The calculated valence band is an almost perfect parabola, its wavefunction is nearly isotropic, and its Fermi surface deviates from a perfect sphere by only 0.2%. These deviations of the Fermi surface from a perfect sphere necessarily lead to a further, albeit small, reduction of the discontinuity when $n(p)$ is orientationally averaged.

Many-body effects introduce a much larger reduction of the discontinuity at the Fermi surface. This is known as the quasiparticle renormalization factor, $Z_{\mathbf{k}_F}$. Theoretical predictions for $Z_{\mathbf{k}_F}$ using different approximations range from 0.45 to 0.79 for the density considered (see Table I). In general, the renormalization factor $Z_{\mathbf{k}_F}$ is related to the self-energy $\Sigma_{\nu, \nu}(k, \omega)$ via $Z_{\mathbf{k}_F} = (1 - \partial \Sigma_{1,1}(\mathbf{k}_F, \omega) / \partial \omega |_{\omega=\epsilon_F})^{-1}$, $\Sigma = \Sigma^{e-e} + \Sigma^{e-p}$ containing the electron-electron interactions, Σ^{e-e} , and the electron-phonon effects, Σ^{e-p} . For HEG the discontinuity in the momentum distribution is $\zeta_{\text{HEG}} = Z_{k_F}$. In a jellium-like system such as Na, band-structure effects and many-body correlations can be factorized so that $\zeta_{\text{Na}} = |\tilde{\phi}_{\nu=1, \mathbf{k}_F}^{\mathbf{G}=0}|^2 Z_{\mathbf{k}_F}$ with a renormalization factor very close to the value for HEG at the same density, if phonon effects can be neglected.

To determine $Z_{\mathbf{k}_F}$ theoretically, we performed pseudopotential diffusion QMC [10, 11] calculations of bulk

sodium based on a Slater-Jastrow (SJ) wavefunction using the QMCPACK code, and more precise calculations using backflow (BF) for HEG. Complementary to QMC, we have done a non-self-consistent (one-shot) G_0W_0 calculation [2] starting from the DFT-LDA electronic structure using the ABINIT code.

Within both methods, pseudopotentials are used to describe the core electrons, based on a regular static lattice for the ions, neglecting effects due to electron-phonon coupling. Whereas core correlation effects only give smooth corrections that do not influence the value of the renormalization factor, electron-phonon coupling may lead to a further decrease of $Z_{\mathbf{k}_F}$. However, since the phonon Debye frequency ω_D is small compared to the Fermi energy, main effects of Σ^{e-p} are expected only within a narrow momentum region around p_F , with $\delta p / p_F \lesssim \omega_D / p_F^2 \approx 10^{-2}$. As we will see below, those effects are beyond the resolution of the experiment. The static approximation and the use of pseudopotential should thus be sufficient to obtain the value of $Z_{\mathbf{k}_F}$, whereas they may be less accurate to predict the whole CP.

Experiment A unique bulk-sensitive probe of the momentum density is offered by Compton scattering of x-rays [12]. The experiment measures the spectra of x-rays scattered by an electron system. When the energy transferred to the electron is much larger than its binding energy, the so-called impulse approximation (IA) is valid and the measured spectrum is related to the CP, which in isotropic average normalized to one electron is

$$J(q) = \frac{3}{8\pi p_F^3} \int_{4\pi} d\Omega \int_{|q|}^{\infty} p n(\mathbf{p}) dp. \quad (1)$$

Here q is the component of the ground-state momentum of the electron projected onto the scattering vector. Assuming an isotropic system, $n(p)$ can thus be extracted by a differentiation of the CP,

$$n(p) = -\left. \frac{2p_F^3}{3p} \frac{dJ(q)}{dq} \right|_{q=p}. \quad (2)$$

For the non-interacting HEG the CP is an inverted parabola $J(q) = \frac{3}{4p_F^3}(p_F^2 - q^2)$ for $q < p_F$ and vanishes for $q > p_F$ ($p_F = 0.49(1)$ a.u. for Na). Many-body effects promote a part of the electrons from below to above p_F . The CP, while being always continuous, should retain a kink, i.e. a discontinuity in the first derivative at k_F . Measuring the CP accurately allows the extraction of $n(p)$ by using Eq. (2). The determination of Z_{k_F} via x-ray Compton scattering has been a long-standing goal of many scientists [12]. The simultaneous requirements of extremely high momentum resolution and statistical accuracy as well as difficulties in separating band-structure and correlation effects have made such attempts difficult, leading to anomalously low values of e.g. $Z_{k_F}^{\text{Li}} = 0.1(1)$ for Li ($r_s = 3.25$) [13]. Promising results were given

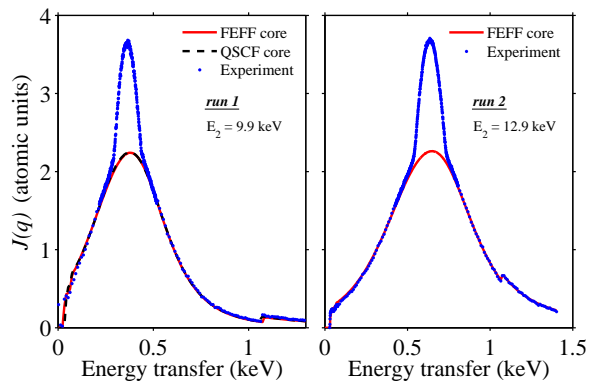


FIG. 2: (Color online) The measured x-ray-scattering spectra from Na as a function of energy transfer, for both experimental runs. The experimental spectra consist of overlapping valence and core contributions. Theoretical core contributions are shown for both QSCF and FEFFq treatments.

for Al ($r_s = 2.07$) [14] by comparisons with an analytical model of $n(p)$ with an adjustable Z_{k_F} [13], giving the best agreement with $Z_{k_F}^{\text{Al}} \approx 0.7$. This determination however assumed a specific shape of $n(p)$ and thus was not model-independent. Our choice of a HEG-like system of Na combined with ultra-high resolution measurements allows us to accurately determine the $n(p)$ and $Z_{k_F}^{\text{Na}}$ in a model-independent way.

The experiments were performed at the beamline ID16 [15] of the European Synchrotron Radiation Facility on polycrystalline sodium. The spectrometer was based on a Rowland circle with spherically bent analyzer crystals with a Bragg angle of 89° . The measurements were done by changing the incident-photon energy E_1 and observing the flux of scattered photons into a fixed scattering angle 2θ at a fixed energy E_2 . We used two different configurations and photon-energy ranges to verify the result in two independent ways. In the first experiment (*run 1*), we used a single Si(555) analyzer crystal, $E_2 = 9.9$ keV, $2\theta = 147^\circ$ and $E_1 = 9.9$ – 11.0 keV. In the second experiment (*run 2*), two Si(880) analyzers were used, with $E_2 = 12.9$ keV, $2\theta = 149^\circ$ and $E_1 = 12.9$ – 14.0 keV. The sample was prepared in a glove box and transported to the beamline within an argon atmosphere and pumped into a vacuum of 10^{-6} mbar. There was no observable degradation of the sample when it was inspected after the experiment. The measured signal was corrected for sample self-absorption as well as changes in the incident photon flux and the spectra were measured repeatedly to identify any possible instabilities during the experiment. None were found and the spectra were finally averaged.

The measured spectra as a function of energy transfer are shown in Fig. 2. The Na L edges are seen at 30–60 eV, and K edge at 1.07 keV. In *run 1* the CP is centered at an energy transfer of 365 eV and in *run 2* at 645 eV. Since our interest is in the valence-electron CP,

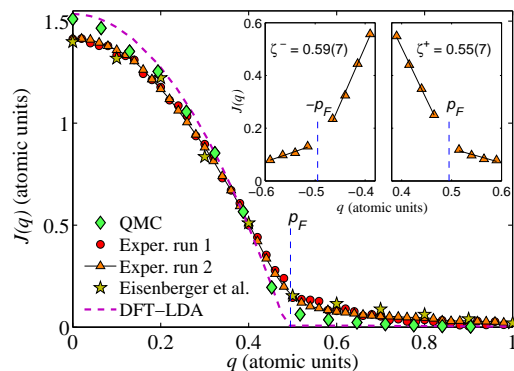


FIG. 3: (Color online) The experimentally determined valence CPs from the two runs (averaged over $q < 0$ and $q > 0$), compared to the results of Eisenberger *et al.* [9], and to the QMC CP in the (100) direction. Inset: zoom on the discontinuity (points) and the linear fits to the CP around the Fermi momentum. Both runs give the same result within the errorbars, the fits shown here are from *run 2*.

the core contribution has to be subtracted first. Since the IA is not strictly valid for the core-electron spectra in these experiments, we calculated them with two independent methods: using i) the quasi-self-consistent field (QSCF) approximation [16] and ii) the real-space multiple scattering approach with the FEFF program [17] with modifications for calculating the momentum-dependent scattering cross-section [18]. The differences between the two approaches are negligible. The core contribution can then be reliably subtracted from the experimental spectra. The spectra can now be converted into the CP [19]; for each energy transfer we can evaluate the scattering-electron momentum component q and the measured intensity is related to the probability of finding the electron with that q .

A finite experimental accuracy in the determination of q will introduce a broadening of any sharp features in the experimental data. This uncertainty is caused in the present experiments by the spread of scattering angles of the detected radiation. This geometrical contribution to the q -resolution was $\Delta q = 0.018$ a.u. (*run 1*) and $\Delta q = 0.027$ a.u. (*run 2*) full-width-at-half-maximum (FWHM). Final-state effects [20, 21], i.e. the interaction of the scattering electron and the rest of the electron gas, are known to cause further broadening of the measured valence Compton profiles. We calculated the magnitude of this broadening [20], and found it to be effectively an additional Gaussian smoothing of 0.08 a.u. (*run 1*), and 0.03 a.u. (*run 2*) (FWHM). This combined with the geometrical resolutions yields effective experimental q -resolutions of 0.08 a.u. (*run 1*) and 0.04 a.u. (*run 2*).

Results and discussion The result of the experiment, after the analysis described above, is the valence CP shown in Fig. 3. The valence CP of a real metal in general deviates from the jellium parabola due to two reasons: (i)

correlation modifies the $n(p)$ introducing tails for $p > p_F$, and (ii) electron-ion interaction modifies the overall wavefunction and induces tails for $p > p_F$ due to core-orthogonalization and the high-momentum components $\tilde{\phi}_{\nu\mathbf{k}}^{\mathbf{G}\neq 0}$. As discussed above, the valence electron wavefunction of Na is fully contained inside 1BZ and is highly free-electron-like, with negligible high-momentum components. The band structure only leads to small ($\lesssim 3\%$) lowering of the momentum distribution for $p < p_F$, as can be seen in the difference between the ideal-Fermi-gas and the DFT-LDA results in Fig. 1. For this reason, we can compare the experimental momentum distribution and the CP to those of HEG after taking these small corrections into account.

In Fig. 3, the Fermi momentum can be directly seen as the discontinuity of the valence CP derivative. From the experimental data we deduce $p_F = 0.49(1)$ a.u. (LDA value 0.481 a.u.). The best determination of the magnitude of the discontinuity at the Fermi surface is provided by linear fits to the measured points in the immediate vicinity of p_F . An inset to Fig. 3 shows these fits, here for both negative and positive q from the higher- q -resolution *run 2*. The difference of the slopes for the two sides gives $\zeta^- = 0.59(7)$ and $\zeta^+ = 0.55(7)$, which allows us to quote the average value as $\zeta_{\text{exp}}^{\text{Na}} = 0.57(7)$. The errorbar is based on the statistical noise of $J(q)$ and the uncertainty of p_F (cf. Eq. (2)). Using the pure band-structure value in LDA, $|\tilde{\phi}_{\nu=1,\mathbf{k}_F}^{\mathbf{G}=0}|^2 = 0.98$, we deduce the experimental $Z_{k_F} = \zeta_{\text{exp}}^{\text{Na}}/|\tilde{\phi}_{\nu=1,\mathbf{k}_F}^{\mathbf{G}=0}|^2 = 0.58(7)$. We simulated the effect of the finite experimental q -resolution by convoluting the QMC CP with the resolution function of *run 2*, and repeating the analysis described above. The result was an effective lowering of $\zeta_{\text{QMC}}^{\text{Na}}$ by 0.02. Since this effect is smaller than our errorbar of 0.07, no further correction to the final experimental result was found necessary.

The momentum distribution can be calculated from the experimental CP using Eq. (2) and is shown in Fig. 1. In the differentiation, the effect of statistical noise increases and thus we only show the result after averaging the values of $p < 0$ and $p > 0$, as well as averaging adjacent measured points. Due to this, the quantitative determination of ζ is better done by directly analyzing the CP as described above. However, the trend of Table I is clearly seen also in Fig. 1 and the experimental $n(p)$ is consistent with the obtained $\zeta_{\text{exp}}^{\text{Na}}$.

We have also calculated the CP by QMC in the (100) direction (Fig. 3); small differences with respect to the experiment remain. Further calculations are necessary to study if the inclusion of core electrons or phonon effects are necessary to reduce the residual discrepancy between theory and experiment in the CP. In Fig. 1, we show the resulting direction-averaged $n(p)$. Finite-size corrections [22] are important to determine the structure around p_F , in particular to obtain the jump at the Fermi surface, $\zeta_{\text{QMC}}^{\text{Na}} = 0.68(2)$. Within the QMC approach, we can

determine bare band-structure effects by turning off the explicit electron-electron correlations in the underlying many-body wavefunction which yields a band-structure contribution $|\tilde{\phi}_{\nu=1,\mathbf{k}_F}^{\mathbf{G}=0}|^2 = 0.97(1)$ compatible with that of DFT-LDA. We therefore obtain $Z_{k_F}^{\text{Na}} = 0.70(2)$, in agreement with QMC calculations of HEG using the same type of wavefunctions (SJ). Within HEG, we have performed calculations using more accurate Slater-Jastrow backflow (BF) wavefunctions which indicate a slightly lower value, $Z_{k_F}^{\text{HEG}} = 0.66(2)$.

From the G_0W_0 self-energy, we directly obtain $Z_{k_F} = (1 - \partial\Sigma_{1,1}(\mathbf{k}_F, \omega)/\partial\omega|_{\omega=\epsilon_F})^{-1} = 0.65(1)$. In order to determine the jump in $n(p)$, we further need the quasiparticle weight which, within G_0W_0 , coincides with the Kohn-Sham orbital of the DFT-LDA calculation at the Fermi energy, and we get $\zeta_{G_0W_0}^{\text{Na}} = 0.64(1)$. The momentum distribution within G_0W_0 is very close to the QMC result.

The agreement between QMC-BF and G_0W_0 is remarkable. Furthermore, within both theories band-structure effects can be factorized from correlations within the accuracy of the calculation, which enables a direct comparison with HEG. In Table I, we summarize our experimental and theoretical results on Z_{k_F} and compare them to various theoretical results obtained for HEG. On theoretical grounds, QMC-BF is considered to give the most precise result. Together with G_0W_0 , it is in reasonable agreement with the experiment.

Our experimental and theoretical values clearly exclude two different classes of approximation, and thus resolve a long-standing theoretical controversy. Whereas the so-called on-shell approximation of the RPA [4, 5] leads to an underestimation of Z_{k_F} , fully self-consistent GW calculations [6] overestimate its value. The latter result shows in particular that the use of the theoretically more appealing conserving approximation (GW) does not result in an improved description of spectral quantities compared to non-self-consistent (G_0W_0) treatments.

Conclusions We have determined the momentum distribution of Na valence electrons experimentally and theoretically. In particular, we have related the discontinuity at the Fermi level to the quasiparticle renormalization factor of HEG at $r_s = 3.99$, giving a long-sought reference value for this fundamental quantity.

Beamtime was provided by the ESRF. The authors would like to thank Gy. Vankó, G. Monaco, R. Verbeni, H. Müller and C. Henriquet (ESRF) for expert advice and assistance. J.A.S., T.P. and K.H. were supported by the Academy of Finland contract No. 1127462. Computer time was provided by the DOE Incite allocation. Funding was provided by Endstation.

-
- [1] P. Nozières, *Theory of Interacting Fermi Systems* (Benjamin, New York, 1964).
- [2] L. Hedin, Phys. Rev. **139**, A796 (1965).
- [3] T. Rice, Ann. Phys. (N.Y.) **31**, 100 (1965).
- [4] E. Pajanne and J. Arponen, J. Phys. C: Solid State Phys. **15**, 2683 (1982).
- [5] J. Lam, Phys. Rev. B **3**, 3243 (1971).
- [6] B. Holm and U. von Barth, Phys. Rev. B **57**, 2108 (1998).
- [7] L. J. Lantto, Phys. Rev. B **22**, 1380 (1980).
- [8] Y. Takada and H. Yasuhara, Phys. Rev. B **44**, 7879 (1991).
- [9] P. Eisenberger, L. Lam, P. M. Platzman, and P. Schmidt, Phys. Rev. B **6**, 3671 (1972).
- [10] W. M. C. Foulkes, L. Mitas, R. J. Needs, and G. Rajagopal, Rev. Mod. Phys. **73**, 33 (2001).
- [11] C. Filippi and D. M. Ceperley, Phys. Rev. B **59**, 7907 (1999).
- [12] M. J. Cooper, P. E. Mijnarends, N. Shiotani, N. Sakai, and A. Bansil, eds., *X-Ray Compton Scattering* (Oxford University Press, Oxford, 2004).
- [13] W. Schülke, G. Stutz, F. Wohlert, and A. Kaprolat, Phys. Rev. B **54**, 14381 (1996).
- [14] P. Suortti, T. Buslaps, V. Honkimäki, C. Metz, A. Shukla, T. Tschentscher, J. Kwiatkowska, F. Maniawski, A. Bansil, S. Kaprzyk, et al., J. Phys. Chem. Solids **61**, 397 (2000).
- [15] R. Verbeni, T. Pylkkänen, S. Huotari, L. Simonelli, G. Vankó, K. Martel, C. Henriquet, and G. Monaco, J. Synchrotron Radiat. **16**, 469 (2009).
- [16] A. Issolah, B. Lévy, A. Beswick, and G. Loupiau, Phys. Rev. A **38**, 4509 (1988).
- [17] J. J. Rehr and R. C. Albers, Rev. Mod. Phys. **72**, 621 (2001).
- [18] J. A. Soininen, A. L. Ankudinov, and J. J. Rehr, Phys. Rev. B **72**, 045136 (2005).
- [19] P. Holm, Phys. Rev. A **37**, 3706 (1988).
- [20] J. A. Soininen, K. Hämäläinen, and S. Manninen, Phys. Rev. B **64**, 125116 (2001).
- [21] C. Sternemann, K. Hämäläinen, A. Kaprolat, A. Soininen, G. Döring, C.-C. Kao, S. Manninen, and W. Schülke, Phys. Rev. B **62**, R7687 (2000).
- [22] M. Holzmann, B. Bernu, V. Olevano, R. M. Martin, and D. M. Ceperley, Phys. Rev. B **79**, 041308(R) (2009).